This is an *Accepted Manuscript*, which has been through the Royal Society of Chemistry peer review process and has been accepted for publication.

Accepted Manuscripts are published online shortly after acceptance, before technical editing, formatting and proof reading. Using this free service, authors can make their results available to the community, in citable form, before we publish the edited article. We will replace this *Accepted Manuscript* with the edited and formatted *Advance Article* as soon as it is available.

You can find more information about *Accepted Manuscripts* in the **Information for Authors**.
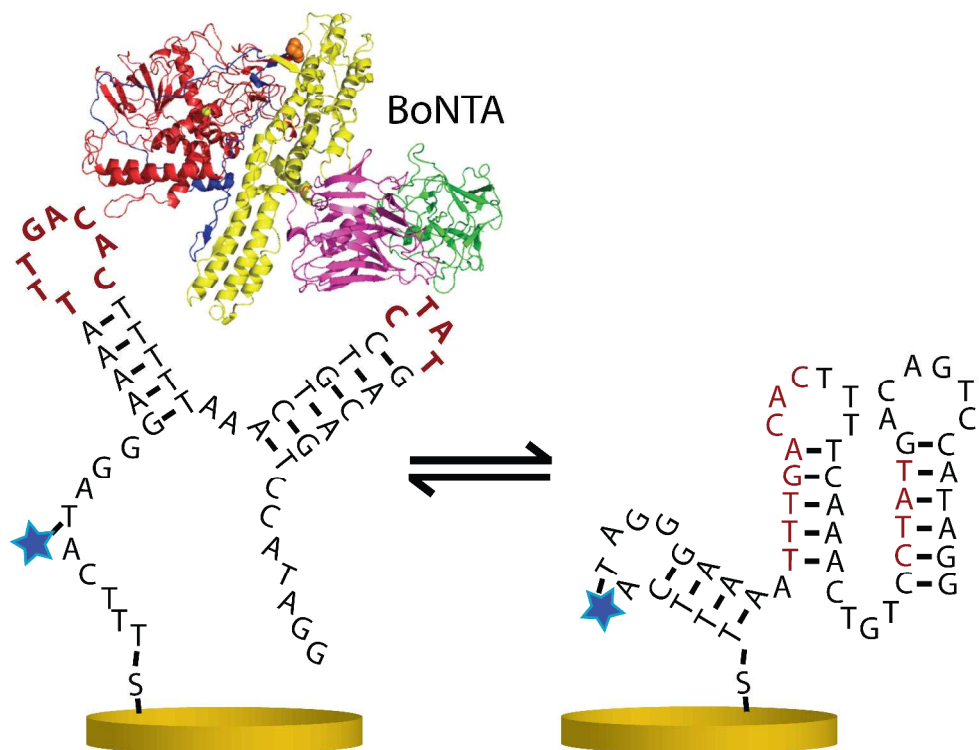
Electrochemical aptamer biosensors for ricin and botulinum neurotoxins are reported, with strategies for generalized biosensor design.

Chemical Communications

COMMUNICATION

Electrochemical Aptamer Scaffold Biosensors for Detection of Botulism and Ricin Toxins

Lisa Fetter[a,†], Jonathan Richards[a,†], Jessica Daniel[a], Laura Roon[a], Teisha J. Rowland[b], Andrew J. Bonham[a,*]

Protein toxins present considerable health risks, but detection often requires laborious analysis. Here, we developed electrochemical aptamer biosensors for ricin and botulinum neurotoxins, which display robust and specific signal at nanomolar concentrations and function in dilute serum. These biosensors may aid future efforts for the rapid diagnosis of toxins.

Biological, protein-based toxins can be threats to human health and safety, but current identification methodologies are often not well suited for timely response. One key example is botulism, a potentially fatal disease caused by the protein-based botulinum neurotoxin, which the bacteria *Clostridium botulinum* produces[1]. This bacteria is common in soil and water, and its toxin is primarily transferred to humans through improperly prepared food or needle transfer in drug use[1]. The botulinum toxin also has potential use as a biological warfare agent[2]. Unfortunately, diagnosis of botulism often relies on mouse inoculations or ELISA tests, which have limited utility given a typical turnaround time of 2-5 days[3]. Given the rapid onset of disease symptoms and potentially fatal toxicity, it would be of considerable benefit to offer a rapid screening instrument to improve food safety and medical diagnosis. Similarly, the protein-based toxin ricin, which is produced by the castor oil plant (*Ricinus communis*), has high human toxicity (with a median lethal dose of <1 mg/kg) and has been used as a biological warfare agent[4]. Again, onset of symptoms (typically within 6 to 12 hours) is rapid compared to the timescale of accurate identification[5].

One recent solution to the need for specific, rapid diagnostics has been biosensors, which use biological interactions as the basis for their sensing elements[6]. A successful class of these

biosensors is electrochemical DNA-based (E-DNA) biosensors[7] (**Figure 1**). E-DNA biosensors rely on the conformational dynamics of an oligonucleotide (i.e., DNA) scaffold with an inserted aptamer. The scaffold typically contains an electrochemically active moiety (e.g., methylene blue dye) and is bound to an electrode surface (e.g., a ceramic-patterned gold electrode) that is subjected to voltammetric analysis. Interactions between the DNA scaffold and the target induce DNA conformation changes that, due to the altered position and dynamics of the electrochemically active moiety, cause characteristic changes in the observed current output[8]. This class of biosensors has been used for sensitive detection of oligonucleotides[8], small molecule drugs[9], antibodies[10], and DNA-binding proteins[11]. Additionally, E-DNA biosensors can function in complex media and have been used to detect physiologically-relevant target levels in rats[7,12]. E-DNA biosensors also require no reagents and can provide quantitative detection in minutes, making rapid and remote on-site detection feasible. Together, these characteristics make the E-DNA platform well suited for the point-of-care detection of biological toxins in complex media, such as foods and blood.

Here, we present a general strategy that enables the creation of E-DNA biosensors directed against protein targets of interest based on the incorporation of aptamers into a conformational-switching oligonucleotide scaffold (**Figure 1**). We used this strategy with an existing aptamer for ricin chain A (RTA)[13] and a novel aptamer we selected that binds botulinum neurotoxin variant A (BoNTA) to generate effective E-DNA biosensors against these protein-based toxins.

For the generation of the BoNTA aptamer, recombinant, non-toxic BoNTA[14] was biotinylated (Chromalink Biotin One-Shot Antibody-Labeling kit, Solulink) and bound to magnetic streptavidin-coated beads (Pierce). These beads were then used as a selection target for a library of DNA oligonucleotides incorporating unnatural nucleobases (X-Aptamers kit, AM Biotechnologies)[15]. Briefly, the selection procedure began with a library of ~10^8 oligos with a variable region of 30 nucleotides. A negative selection against unconjugated beads was

a. *Department of Chemistry, Metropolitan State University of Denver, Denver, CO 80204.*
b. *Cardiovascular Institute and Adult Medical Genetics Program, University of Colorado Denver Anschutz Medical Campus, Aurora, CO 80045.*
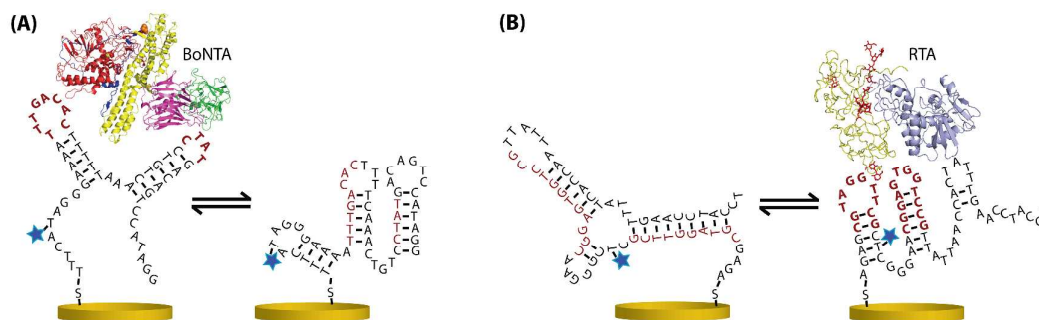† These authors contributed equally to this manuscript.
* Corresponding author: abonham@msudenver.edu

Chemical Communications

COMMUNICATION

Figure 1. Schematic of aptamer scaffold electrochemical DNA (E-DNA) biosensors. A specific target-binding aptamer (red) is inserted into an oligonucleotide scaffold (black). A thiol group (S) on the scaffold attaches it to the gold electrode surface (yellow). The position and dynamics of a methylene blue molecule (blue star, attached to the scaffold) relative to the electrode surface changes in response to aptamer-target binding, producing a measurable electrical current change. Biosensors directed against botulism toxin (BoNTA, **A**) and ricin toxin (RTA, **B**) are shown.

performed, followed by a positive selection against BoNTA-conjugated beads and then a procedure where oligos were exposed to soluble BoNTA, followed by conjugation of the complex to beads and a final selection. The resultant selected oligonucleotides were characterized by high-throughput sequencing, identifying 16 putative aptamers (sequences in **Supporting Table 1**). These were synthesized as 5'-Cy3 conjugates and binding was confirmed via gel mobility shift assays with BoNTA (**Supporting Figure 1**). One aptamer (identified as 2.5 in **Supporting Table 1**) displayed nanomolar affinity for BoNTA (apparent K_D 10 $\pm$ 4 nM) and was chosen for further efforts.

We used this novel BoNTA aptamer and the previously identified RTA aptamer as the core sequences for our biosensor generation strategy, which is based on optimizing the DNA scaffold (with aptamer insert) towards two isoenergetic folded states (using Quikfold secondary structure prediction routines)[16]. One of these states folds the aptamer and scaffold into the predicted secondary structure of the binding-capable form while the other state intentionally disrupts the stem-loop structures of the aptamer that are expected to be required for efficient binding. This strategy builds upon methods we have optimized for optical biosensors against transcription factor targets[17].

Our strategy to optimize the DNA scaffolds for the BonTA and RTA aptamers had each aptamer initially divided into predicted essential and dispensable elements. Essential elements included the identity of bases in loops in the aptamer sequence and the distance between loops (as these disordered loops typically form the target binding regions of aptamers[18]), while dispensable elements included the identity of the bases in the stems and bases flanking the main aptamer sequence. To generate DNA biosensors occupying both the binding-

capable and disrupted, non-binding folded states at equilibrium, an iterative process was employed wherein the dispensable elements for each aptamer were sequentially replaced with novel scaffold sequences. To promote a disrupted state, the bases flanking core aptamer sequences needed to be at least partially complementary to the core loops to generate new stem structures that can bind the aptamer loop bases, preventing them from forming target interactions. During this process, the DNA scaffold designs were assessed for both binding and disrupted, non-binding isoenergetic states[17]. The basic designs were then further optimized via addition or substitution of individual bases to stabilize the desired states of the predicted structures.

The predicted secondary structures of our biosensors are shown in **Figure 1** (see **Supporting Table 2** and **Supporting Figure 2** for full sequences and predicted secondary structures and parameters for the biosensors). Each biosensor was synthesized (Biosearch Technologies) with a 5' disulfide for binding to a gold electrode surface, as well as a covalently-incorporated internal methylene blue (appended via amide
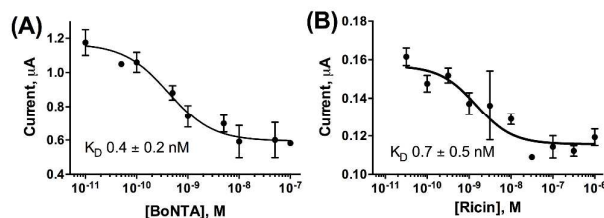
Figure 2. Dose-responsive curves for peak current vs. toxin concentration for botulinum neurotoxin variant A (BoNTA, **A**) and ricin toxin chain A (RTA, **B**). Both E-DNA biosensors displayed robust equilibrium signal change in response to target concentration, with apparent dissociation constant (K_D) values of 0.4 ± 0.2 nM for BoNTA and 0.7 ± 0.5 nM for RTA.
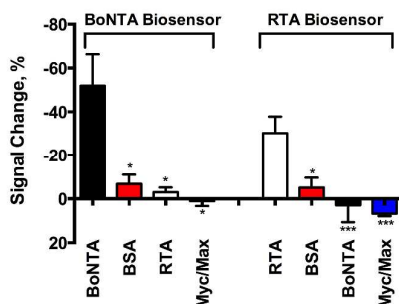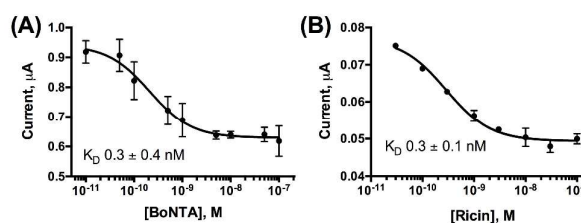
Figure 3. The BoNTA and RTA biosensors display minimal off-target responses when challenged with the non-targeted toxin, non-specific serum protein bovine serum albumin (BSA), or the unrelated DNA-binding protein complex Myc/Max. Student's t-test was performed to compare on-target to off-target response (* for p < 0.05, *** for p < 0.0001).

Figure 4. Dose-responsive curves for the biosensors performed in a mixture containing 10% bovine blood serum (BSA) and 90% 1xPBS. Peak current vs. toxin concentration is shown for botulinum neurotoxin variant A (BoNTA, **A**) and ricin toxin chain A (RTA, **B**). Both E-DNA biosensors display robust equilibrium signal change in response to their respective targets in these complex fluids.

linkage to a modified thymine) to serve as the electrically active reporter. Significant changes in the position and accessibility of the methylene blue in relation to the electrode surface affects the transfer of electrons between the methylene blue and the electrode surface (e.g., increased distance and decreased accessibility results in decreased reported electrical signal)[11]. To ensure a robust difference in reported electrical signal between the two folded states, the methylene blue was attached to a thymine predicted to be significantly different in its flexibility and distance from the electrode surface when comparing the binding-capable state to the non-binding state (in these predictions, the 5' disulfide was used as an estimation of the position of the electrode surface). As target binding causes a shift between the two states, a change in observed current is linked to the structural switch of the scaffold[19].

These biosensors were attached to cleaned gold electrode surfaces via established protocols (see **Supporting Information**)[20]. These biosensors displayed robust baseline response (**Supporting Figure 3**) in 1X PBS buffer (10 mM phosphate, 137 mM NaCl, 2.7 mM KCl, pH 7.4) as well as in a solution of 90% 1X PBS and 10% bovine blood serum (Sigma Aldrich).

The affinity and detection limit of each biosensor was tested via square wave voltammetric scanning of equilibrated solutions containing the respective toxin, atoxic BoNTA or RTA. Biosensors were scanned from -400 mV to 100 mV at 50 mV/sec with 50 mV amplitude, 150 Hz. Under these conditions, a peak in the current was observed at approximately -250 mV for the methylene blue moiety of the biosensor, and this peak current varies with target toxin concentration (**Supporting Figure 3**). Peak current was measured using custom peak-fitting software[12]. For each biosensor, serial equilibration using increasing amounts of toxin followed by peak current measurement fit well to a law of mass action dose-response relationship, giving apparent dissociation constant (K_D) values of 0.4 ± 0.2 nM for BoNTA and 0.7 ± 0.5 nM for RTA (**Figure 2**). These low nanomolar dissociation constants are similar to the binding of other aptamers to protein targets[21–23], with the apparent K_D for our BoNTA sensor being comparable to previously reported K_D

values of approximately 2 nM or 3 nM for other aptamer sensors against BoNTA[24,25] and our RTA sensor being comparable to an earlier RTA aptamer with a K_D of 7 nM[26]. RTA has an LD_{50} in mice of 10 ug/kg via injection, which is approximately 2 nM concentration in blood, suggesting that our RTA biosensor is sufficiently sensitive for the diagnosis of ricin poisoning under real-world, clinical conditions. In contrast, BoNTA is exceptionally toxic, displaying mouse lethality at sub-picomolar concentrations in mice[3], and the BoNTA biosensor presented here is not sensitive at these levels. Improvements upon the design may enable the increased sensitivity needed for medical diagnosis of BoNTA. Thus, these biosensors together represent an important first step towards rapid, electrochemical detection of these targets at medically relevant concentrations.To further establish that the observed dose-response behavior was not due to biosensor degradation or non-specific binding, each biosensor was challenged with off-target proteins. These included the alternative toxin (BoNTA on the RTA biosensor and vice-versa), bovine serum albumin (BSA; to serve as a generic soluble protein), and the c-Myc/Max transcription factor complex (as an example of DNA-binding proteins, which might be expected to interfere with DNA-based biosensors). All off-target proteins were equilibrated at 100 nM concentrations, which gave robust response for the correct target. We found that these off-target interactions were not significantly different from background measurements (**Figure 3**). This agrees with prior efforts to characterize the specificity of E-DNA biosensors[7], suggesting that they have high target specificity.

We further tested both biosensors for function in complex media, which would greatly enhance their utility in diagnostic applications. Each biosensor was tested using the previously described equilibrium titration methodology, but in 10% bovine blood serum with 90% 1X PBS rather than pure PBS buffer. Under this regime, the quantity of solution needed for experimental analysis is less than 20 uL; this is less than the amount of blood available from finger lancet, and consequently could enable point-of-care diagnostic utility by allowing testing without requiring phlebotomy procedures. We observed virtually unchanged apparent dissociation constants for both biosensors in this testing regime (**Figure 4**), with apparent dissociation constant (K_D) values of 0.3 ± 0.4 nM for BoNTA and 0.3 ± 0.1 nM for RTA. This further highlights

Please do not adjust margins **ChemComm**

the sensitivity and specificity of the E-DNA platform in this application, and provides a first step towards diagnostic validation.

The E-DNA biosensors presented here, directed against botulinum and ricin toxins, display rapid, sensitive, and specific detection of their targets. Future efforts will be needed to optimize these biosensors for function in pure serum or whole blood, although both our recently shown methodology based on laminar flow that allows direct interface with whole blood without significant modification of the biosensor[12] and a surface plasmon-based BoNTA biosensor stable in complex fluids over multiple cycles[27] suggest that such optimizations are eminently possible. Given that E-DNA biosensors function with inexpensive, handheld potentiometric detectors[28,29], these optimized biosensors could be used to assess real-world blood and fluid samples, offering an on-site, point-of-care or point-of-contact solution for food safety and health assessment. Moreover, we show that the biosensor generation strategy employed here has promise as a simple and successful way to create biosensors against a variety of arbitrarily-chosen protein targets, allowing expansion of detectable targets to enable multiple sensing applications.

Notes and references

1. J. Sobel, *Clin. Infect. Dis.*, 2005, **41**, 1167–73.
2. S. S. Arnon, R. Schechter, T. V. Inglesby, D. A. Henderson, J. G. Bartlett, M. S. Ascher, E. Eitzen, A. D. Fine, J. Hauer, M. Layton, S. Lillibridge, M. T. Osterholm, T. O'Toole, G. Parker, T. M. Perl, P. K. Russell, D. L. Swerdlow, and K. Tonat, *JAMA*, 2001, **285**, 1059.
3. S. Cai, B. R. Singh, and S. Sharma, 2008.
4. L. G. Doan, *Clin. Toxicol.*, 2004, **42**, 201–208.
5. J. Audi, M. Belson, M. Patel, J. Schier, and J. Osterloh, *JAMA*, 2005, **294**, 2342–51.
6. J. Wang, *Biosens. Bioelectron.*, 2006, **21**, 1887–1892.
7. A. a Lubin, R. Y. Lai, B. R. Baker, A. J. Heeger, and K. W. Plaxco, *Anal Chem*, 2006, **78**, 5671–7.
8. F. Ricci and K. W. Plaxco, *Microchim. Acta*, 2008, **163**, 149–155.
9. J. S. Swensen, Y. Xiao, B. S. Ferguson, A. a Lubin, R. Y. Lai, A. J. Heeger, K. W. Plaxco, and H. T. Soh, *J Am Chem Soc*, 2009, **131**, 4262–4266.
10. A. Vallée-Bélisle, F. Ricci, T. Uzawa, F. Xia, and K. W. Plaxco, *J. Am. Chem. Soc.*, 2012, **134**, 15197–200.
11. A. J. Bonham, K. Hsieh, B. S. Ferguson, A. Valle-Belisle, F. Ricci, H. T. Soh, and K. W. Plaxco, *J. Am. Chem. Soc.*, 2012, **134**, 3346–3348.
12. B. S. Ferguson, D. a Hoggarth, D. Maliniak, K. Ploense, R. J. White, N. Woodward, K. Hsieh, A. J. Bonham, M. Eisenstein, T. E. Kippin, K. W. Plaxco, and H. T. Soh, *Sci. Transl. Med.*, 2013, **5**, 213ra165.
13. B. Wang, C. Guo, M. Zhang, B. Park, and B. Xu, *J. Phys. Chem. B*, 2012, **116**, 5316–22.
14. E. J. Vazquez-Cintron, M. Vakulenko, P. A. Band, L. H. Stanker, E. A. Johnson, and K. Ichtchenko, *PLoS One*, 2014, **9**, e85517.
15. W. He, M.-A. Elizondo-Riojas, X. Li, G. L. R. Lokesh, A. Somasunderam, V. Thiviyanathan, D. E. Volk, R. H. Durland, J. Englehardt, C. N. Cavasotto, and D. G. Gorenstein, *Biochemistry*, 2012, **51**, 8321–3.
16. N. R. Markham and M. Zuker, *Nucleic Acids Res.*, 2005, **33**, W577–81.
17. S. R. Schaffner, K. Norquest, E. Baravik, J. Stephens, L. Fetter, R. M. Masterson, Y. Reyna, and A. J. Bonham, *Sens. Bio-Sensing Res.*, 2014, **2**, 49–54.
18. J. E. Barrick and R. R. Breaker, *Genome Biol.*, 2007, **8**, R239.
19. T. Uzawa, R. R. Cheng, R. J. White, D. E. Makarov, and K. W. Plaxco, *J. Am. Chem. Soc.*, 2010, **132**, 16120–6.
20. A. A. Rowe, R. J. White, A. J. Bonham, and K. W. Plaxco, *J. Vis. Exp.*, 2011, **52**, e2922.
21. X. Fang, A. Sen, M. Vicens, and W. Tan, *ChemBioChem*, 2003, **4**, 829–834.
22. S. E. Osborne, I. Matsumura, and A. D. Ellington, *Curr. Opin. Chem. Biol.*, 1997, **1**, 5–9.
23. E. A. Lamont, L. He, K. Warriner, T. P. Labuza, and S. Sreevatsan, *Analyst*, 2011, **136**, 3884–95.
24. F. Wei and C.-M. Ho, *Anal. Bioanal. Chem.*, 2009, **393**, 1943–8.
25. J. B.-H. Tok and N. O. Fischer, *Chem. Commun. (Camb).*, 2008, 1883–5.
26. J. R. Hesselberth, D. Miller, J. Robertus, and A. D. Ellington, *J. Biol. Chem.*, 2000, **275**, 4937–4942.
27. P. Janardhanan, C. M. Mello, B. R. Singh, J. Lou, J. D. Marks, and S. Cai, *Talanta*, 2013, **117**, 273–80.
28. A. A. Rowe, A. J. Bonham, R. J. White, M. P. Zimmer, R. J. Yadgar, T. M. Hobza, J. W. Honea, I. Ben-Yaacov, and K. W. Plaxco, *PLoS One*, 2011, **6**, e23783.
29. J. R. Mott, P. J. Munson, R. A. Kreuter, B. S. Chohan, and D. G. Sykes, *J. Chem. Educ.*, 2014, **91**, 1028–1036.